A novel calcium looping absorbent incorporated with polymorphic spacers for hydrogen production and CO2 capture

ARTICLE *in* ENERGY & ENVIRONMENTAL SCIENCE · AUGUST 2014

Impact Factor: 20.52 · DOI: 10.1039/C4EE01281J

7 AUTHORS, INCLUDING:

Ming Zhao
Tsinghua University
18 PUBLICATIONS **245** CITATIONS
SEE PROFILE

Jeffrey Shi
University of Sydney
35 PUBLICATIONS **498** CITATIONS
SEE PROFILE

Xia Zhong
University of Sydney
12 PUBLICATIONS **271** CITATIONS
SEE PROFILE

John Blamey
Imperial College London
18 PUBLICATIONS **714** CITATIONS
SEE PROFILE

Energy Fuels **2010,** *24,* 2768–2776 · DOI:10.1021/ef9012449
Published on Web 03/26/2010

energy&fuels
article

Morphological Changes of Limestone Sorbent Particles during Carbonation/Calcination Looping Cycles in a Thermogravimetric Analyzer (TGA) and Reactivation with Steam

Y. Wu,[†,‡] J. Blamey,[‡] E. J. Anthony,[†] and P. S. Fennell*[,‡]

[†]*CanmetENERGY, 1 Haanel Drive, Ottawa, Ontario K1A 1M1, Canada, and* [‡]*Department of Chemical Engineering, Imperial College, South Kensington, London SW7 2AZ, United Kingdom*

Received October 29, 2009. Revised Manuscript Received March 5, 2010

Carbonation and calcination looping cycles were carried out on four limestones in a thermogravimetric analyzer (TGA). The CO_2 carrying capacity of a limestone particle decays very quickly in the first 10 cycles, reducing to about 20% of its original uptake capacity after 10 cycles for the four limestones studied in this work, and it decreases further to 6−12% after 50 cycles. A new steam reactivation method was applied on the spent sorbent to recover the loss of reactivity. The steam reactivation of multi-cycled samples was conducted at atmospheric pressure. Steam reactivation for 5 min at 130 °C of particles that had undergone 10 cycles resulted in an immediate increase (by 45−60% points) in carrying capacity. The morphological changes of limestone particles during the cycling and steam reactivation were studied using both an optical microscope and scanning electron microscopy (SEM). The diameters of limestone particles shrank by about 2−7% after 10 carbonation/calcination cycles, and the particle diameters swelled significantly (12−22% increase) after steam reactivation. These size changes are important for studies of attrition and mathematical modeling of carbonation.

Introduction

CO_2 accounts for the largest amount of anthropogenic greenhouse gas emitted to the atmosphere. Given the abundance of the supply of coal, for both security and economic reasons, it is probable that coal-fired power plants will continue to be the most important method of meeting the increasing global energy demand for the foreseeable future. To prevent the most severe climate change scenarios of greater than 2 °C average global warming, it is therefore necessary to reduce anthropogenic CO_2 emissions.

The reversible carbonation reaction (eq 1), which involves using a limestone-based sorbent, has been proposed for capturing CO_2 (via the forward reaction) from dilute sources (e.g., flue gas from coal-fired power plants) to produce a concentrated CO_2 stream (via the reverse reaction) suitable for geological sequestration and/or enhanced oil or coal bed methane recovery (EOR/ECBM), e.g.[1−6]

$$CaO + CO_2 = CaCO_3 \quad (1)$$

This reaction also has applications within the field of hydrogen production via the sorbent-enhanced water−gas shift reaction.[7] During the calcium looping cycle (CaLC), the sorbent is continuously cycled between a calciner (∼900 °C) and a carbonator (∼650 °C). A 75 kW_{th} CaLC pilot plant has already demonstrated this process on a continuous basis at CanmetENERGY.[8]

While the calcination reaction (the reverse reaction of eq 1) proceeds rapidly to completion under thermodynamically favorable conditions, carbonation is characterized by a fast initial rate followed by an abrupt transition to a very slow reaction rate.[9,10] A major problem associated with the CaLC is that the CO_2 carrying capacity (or absorption capacity) of the sorbent decreases with an increasing number of cycles of carbonation and calcination[11−17] because of sintering of the microstructure within the particle. Grasa and Abanades[14]

*To whom correspondence should be addressed. Telephone: +44-(0)-20-7594-6637. E-mail: p.fennell@imperial.ac.uk.

(1) Blamey, J.; Anthony, E. J.; Wang, J.; Fennell, P. S. The calcium looping cycle for large-scale CO_2 capture. *Prog. Energy Combust. Sci.* **2010**, *36*, 260–279.
(2) Shimizu, T.; Hirama, T.; Hosoda, H.; Kitano, K.; Inagaki, M.; Tejima, K. A twin fluid-bed reactor for removal of CO_2 from combustion processes. *Trans. Inst. Chem. Eng.* **1999**, *77* (part A), 62–68.
(3) Salvador, C.; Lu, D.; Anthony, E. J.; Abanades, J. C. Enhancement of CaO for CO_2 capture in an FBC environment. *Chem. Eng. J.* **2003**, *96*, 187–195.
(4) Abanades, J. C.; Anthony, E. J.; Alvarez, D.; Lu, D. In-situ capture of CO_2 in a fluidized bed combustor. Proceedings of the 17th International (ASME) Conference on Fluidized Bed Combustion, Jacksonville, FL, May 18−21, 2003; Paper 10.
(5) Hughes, R. W.; Lu, D.; Anthony, E. J.; Wu, Y. H. Improved long-term conversion of limestone-derived sorbents for in situ capture of CO_2 in a fluidized bed combustor. *Ind. Eng. Chem. Res.* **2004**, *43* (18), 5529–5539.
(6) Anthony, E. J. Solid looping cycles: A new technology for coal conversion. *Ind. Eng. Chem. Res.* **2008**, *47* (6), 1747–1754.
(7) Harrison, D. P. Sorption-enhanced hydrogen production: A review. *Ind. Eng. Chem. Res.* **2008**, *47* (17), 6486–6501.
(8) Lu, D. Y.; Hughes, R. W.; Anthony, E. J. Ca-based sorbent looping combustion for CO_2 capture in pilot-scale dual fluidized beds. *Fuel Process. Technol.* **2008**, *89*, 1386–1395.
(9) Barker, R. Reversibility of the reaction $CaCO_3 = CaO + CO_2$. *J. Appl. Chem. Biotechnol.* **1973**, *23* (10), 733–742.
(10) Silaban, A.; Harrison, D. P. High temperature capture of carbon dioxide: Characteristics of the reversible reaction between CaO(s) and CO_2(g). *Chem. Eng. Commun.* **1995**, *137*, 177–190.
(11) Abanades, J. C.; Alvarez, D. Conversion limits in the reaction of CO_2 with lime. *Energy Fuels* **2003**, *17* (2), 308–315.
(12) Abanades, J. C.; Anthony, E. J.; Lu, D. Y.; Salvador, C.; Alvarez, D. Capture of CO_2 from combustion gases in a fluidized bed of CaO. *AIChE J.* **2004**, *50*, 1614–1622.
(13) Wang, J. S.; Anthony, E. J. On the decay behavior of the CO_2 absorption capacity of CaO-based sorbents. *Ind. Eng. Chem. Res.* **2005**, *44* (3), 627–629.

undertook an extended series of trials and found that there is a residual carrying capacity remaining after 500 cycles. They also proposed the following semi-empirical equation (eq 2) to describe the experimental results:

$$X_N = \frac{1}{\frac{1}{1 - X_\infty} + kN} + X_\infty \quad (2)$$

In eq 2, X_∞ is the residual carrying capacity and k is the deactivation constant, which increases with more severe calcination conditions (i.e., longer times and/or higher temperatures). It has been established that hydration of spent sorbent, with either high-pressure steam[18−21] or even moist air,[22] is able to reactivate the capacity of the sorbent for CO_2 capture after it has been cycled, by regenerating its microstructure. A new steam reactivation apparatus was developed in this work. The steam reactivation of samples that had undergone multiple cycles of calcination and carbonation was conducted at atmospheric pressure. The aims of this study were to better understand sorbent behavior during repeated carbonation/calcination cycles and steam reactivation, by investigating particle size changes associated with the repeated cycles and the subsequent reactivation process. Such changes are important for carbonation process modeling, in that they affect the porosity of a particle; they are also important for studies of particle attrition, particularly when changes in particle size are used to infer that attrition of particles has occurred. The study also investigated the rate of hydration of particles during steam reactivation.

Experimental Section

Limestone Samples. Four prescreened limestone samples from different geological areas were used in this study: namely, Purbeck (PB, particle size of 0.71−1.00 mm), from southern England, Katowice (KW, particle size of 0.40−0.80 mm), from Poland, Havelock (HL, particle size of 0.71−1.00 mm), from New Brunswick, Canada, and Kelly Rock (KR, particle size of 0.60−0.80 mm), from Nova Scotia, Canada. Some KW and KR samples were further rescreened to 0.71−0.8 mm, and additional tests were conducted on particles of this size range. The X-ray fluorescence (XRF) analyses of the samples investigated are given in Table 1. HL and KW are quite pure limestones, while KR and PB contain higher concentrations of impurities, mainly SiO_2. Importantly, the SiO_2 contained within the PB particles is comprised of individual flints rather than being spread evenly through the particles. This was readily seen by examining crushed samples.

Table 1. XRF Analyses of Limestone Samples (wt %)

component	HL	KR	KW	PB
SiO_2	1.36	2.95	0.85	4.32
Al_2O_3	0.57	0.74	0.24	0.56
Fe_2O_3	0.19	0.32	0.09	0.25
CaO	54.04	52.43	54.10	52.17
MgO	1.27	0.47	0.89	1.47
Na_2O	n/a	< 0.096	< 0.2	n/a
K_2O	0.09	0.21	0.06	0.13

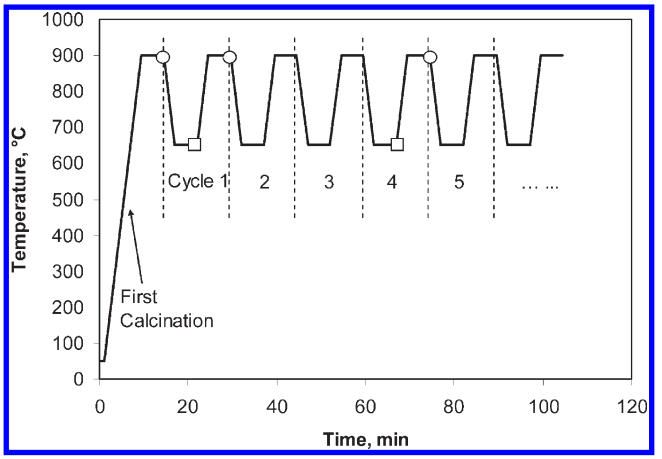

Figure 1. Temperature program for calcination/carbonation cycles in TGA: (○) photomicrographs taken where the calcination process is complete and (□) photomicrographs taken where the carbonation process is complete.

Carbonation/Calcination Cycles. The carbonation and calcination cycles were carried out in a Perkin-Elmer Pyris 1 thermogravimetric analyzer (TGA). The reactive gas flow rates were controlled by two rotameters and one mass flow controller, at a total flow rate of ∼120 mL/min with a CO_2 concentration of 15% (N_2 + He balance). The flow rate and CO_2 concentration were kept unchanged in both carbonation and calcination stages throughout the study, unless otherwise indicated. Temperatures for the calcination and carbonation reactions were set at 900 and 650 °C, respectively. A calcination temperature of 950 °C was used for a limited number of tests with HL limestone. Figure 1 shows the typical temperature program for the carbonation and calcination cycles in the TGA. Both calcination and carbonation durations were 5 min. Examination of the TG profile showed that the rate of calcination was sufficiently fast that the reaction proceeded to completion in ∼1 min, while 5 min of carbonation was sufficient for the transition from the fast (kinetically-controlled) reaction to the slow (diffusion-controlled) reaction, with both findings in agreement with the literature.[10,14,23] Typically, 20−50 cycles were carried out for each sample.

Image Capture and Analysis. To investigate the changes in particle size during multiple carbonation and calcination cycles,

(14) Grasa, G. S.; Abanades, J. C. CO_2 capture capacity of CaO in long series of carbonation/calcination cycles. *Ind. Eng. Chem. Res.* **2006**, *45* (26), 8846–8851.
(15) Fennell, P. S.; Pacciani, R.; Davidson, J. F.; Dennis, J. S.; Hayhurst, A. N. The use of limestone particles for the capture of CO_2: Its initial reactivity and loss of reactivity after repeated cycles of calcination and carbonation. Proceedings of the 19th International Conference on Fluidized Bed Combustion, Vienna, Austria, May 2006; pp 311−320, ISBN 3-200-00645-5.
(16) Fennell, P. S.; Pacciani, R.; Dennis, J. S.; Davidson, J. F.; Hayhurst, A. N. The effects of repeated cycles of calcination and carbonation on a variety of different limestones, as measured in a hot fluidized bed of sand. *Energy Fuels* **2007**, *21* (4), 2072–2081.
(17) Grasa, G.; Abanades, J. C.; Alonso, M.; Gonzalez, B. Reactivity of highly cycled particles of CaO in a carbonation/calcination loop. *Chem. Eng. J.* **2008**, *137*, 561–567.
(18) Manovic, V.; Anthony, E. J. Steam reactivation of spent CaO-based sorbent for multiple CO_2 capture cycles. *Environ. Sci. Technol.* **2007**, *41*, 1420–14255.
(19) Manovic, V.; Anthony, E. J. Sequential SO_2/CO_2 capture enhanced by steam reactivation of a CaO-based sorbent. *Fuel* **2008**, *87* (8−9), 1564–1573.
(20) Manovic, V.; Anthony, E. J.; Lu, D. Y. Sulphation and carbonation properties of hydrated sorbents from a fluidized bed CO_2 looping cycle reactor. *Fuel* **2008**, *87*, 2923–2931.
(21) Manovic, V.; Lu, D.; Anthony, E. J. Steam hydration of sorbents from a dual fluidized bed CO_2 looping cycle reactor. *Fuel* **2008**, *87*, 3344–3352.
(22) Fennell, P. S.; Davidson, J. F.; Dennis, J. S.; Hayhurst, A. N. Regeneration of sintered limestone sorbents for the sequestration of CO_2 from combustion and other systems. *J. Energy Inst.* **2007**, *80* (2), 116–119.
(23) Manovic, V.; Charland, J.-P.; Blamey, J.; Fennell, P. S.; Lu, D. Y.; Anthony, E. J. Influence of calcination conditions on carrying capacity of CaO-based sorbent in CO_2 looping cycles. *Fuel* **2009**, *88*, 1893–1900.

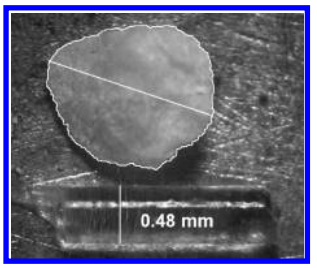

Figure 2. Optical photomicrograph of a limestone particle and quartz rod. The major axis and the boundary of the particle were drawn using the Scion Image software.

single limestone particles (typically 0.6−2.0 mg) were used. The limestone particle was held in a platinum sample pan in the TGA. Photomicrographs of the particles were captured with the help of an optical microscope (Seben Stereo Microscope Incognita III) and an electronic eyepiece (Hangzhou Opto Electronics MD 130). Figure 2 shows an example of the photomicrographs produced. A piece of quartz rod (with a known and constant diameter of 0.48 mm) was placed in the sample pan as a reference, with the limestone particle at the beginning of the TGA run. Care was taken to ensure that the particle did not change orientation throughout an experiment.

Images of the sample were typically taken after the first calcination, the 1st cycle, the 4th cycle, the 10th cycle, and the 12th cycle, as indicated by the symbols shown in Figure 1. For a limited number of experiments, an additional image was taken after allowing the experiment to proceed to the 50th cycle. The majority of the images were captured after the calcination period in a given cycle; however, images after the carbonation period in the same cycle were taken for selected samples (as shown in Figure 1). For each sample, the first photomicrograph was always taken for the original limestone particle before any calcination took place. Subsequently, the limestone (or cycled sorbent) was then heated at 100 °C/min to 900 °C (the calcination temperature) and held for 5 min to ensure complete calcination. A number of cycles of carbonation and calcination could then be conducted. When the aim was to investigate a particle in the calcined form, after 4 min had elapsed (when the weight change always showed complete calcination had occurred), the CO_2 flow to the TGA was turned off to avoid recarbonation from taking place during cooling. The sorbent was then cooled from 900 to 50 °C at 200 °C/min. The sample pan was removed from the TGA, and a set of photomicrographs of the calcined sample was taken. When the image was taken after the carbonation period, the sorbent was cooled from 650 to 50 °C at 200 °C/min, with the CO_2 continuing to flow during the cooling period.

To analyze the photomicrographs, the computer program "Scion Image" was used. The diameter of the major axis of the particle (linear length) was accurately measured for each image by reference to the known diameter of the quartz rod. By manually drawing around the boundary of the particle, the built-in measuring tool of the software could calculate the area encapsulated. Therefore, the equivalent diameter (i.e., the diameter of a spherical particle that would yield the same projected area) of the particle could be calculated. An implicit assumption in this study is that changes in diameter are uniform in all directions. To ensure that the drawing around the particle did not introduce any substantial errors, the procedure was conducted a number of times for the same image; a number of repetitions were also conducted on different particles to check for consistency and reproducibility. Particles were measured in the same orientation and at approximately the same location in the field of view of the microscope, particularly for all measurements of the same particle. This meant that only very minor changes in the focus, etc., of the microscope were necessary within an experiment, so that measurements were consistent.

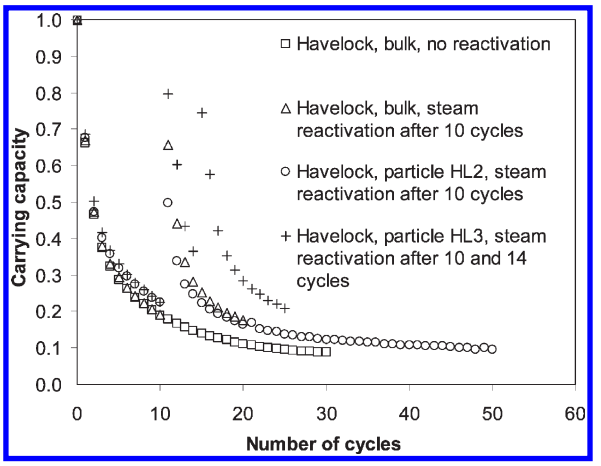

Figure 3. Effect of steam reactivation on CO_2 carrying capacity for HL limestone. Calcination temperature, 900 °C, for 5 min; carbonation temperature, 650 °C, for 5 min; p_{CO_2}, 0.015 MPa; steam temperature, 130 °C (p_{H_2O}, 0.1 MPa), for 5 min.

Figure 2 shows how the width of the quartz rod, used as an internal calibration standard, the linear length, and the area of the particle on the screen were drawn and measured by the software.

Steam Reactivation. Reactivation of the cycled samples was carried out in a steam hydrator, which is a horizontal glass chamber (23 mm inner diameter) connected to a steam generator. The steam generator is a vertical stainless-steel tube ($^1/_4''$ outer diameter), fed by a high-performance liquid chromatography (HPLC) pump with liquid water at a rate of 3.5 mL/min, which corresponded to a flow rate of 6.5 L/min of steam (at 130 °C and atmospheric pressure). The exterior of the hydrator was heated using electrical heating tape, and the steam temperature in the hydrator was controlled at ∼130 °C to avoid condensation. The temperature inside the hydrator was measured at a position close to the pan using a type K thermocouple. The outlet of the hydrator is a cone and socket, reducing to a short length (∼50 mm) of 4 mm inner diameter glass tube to increase the local velocity of the steam leaving the hydrator, thereby preventing the ingress of ambient air. The socket could be rapidly connected and disconnected from the hydrator to effect access to the particles. Typically, after 10 cycles of carbonation and calcination, the sample (together with the pan) was removed from the TGA (as indicated above, CO_2 flow was shut off 1 min before the cooling stage to prevent recarbonation of the sample in the TGA), put into a crucible boat, transferred immediately into the hydrator, and reactivated in steam for 5 min. After steam reactivation, the sample was taken out of the hydrator rapidly and placed back in the TGA for more cycling. In the majority of reactivation experiments, a bulk sample (∼20 mg) was used in the TGA, although some single-particle reactivation experiments were also carried out on HL samples for the purpose of capturing particle images prior to further cycling.

Scanning Electron Microscopy (SEM) Observation. The morphologies of the samples were also examined by SEM using a Hitachi TM-1000 tabletop microscope with 15 kV of accelerating voltage. With this instrument, the sample particles are placed on an adhesive carbon disk and can be observed directly without additional preparation; i.e., there is no requirement to coat the sample with metal before observation. HL limestone samples, having undergone different numbers of cycles with or without steam hydration, were examined by SEM.

Results and Discussion

Decay of the Carrying Capacity and the Effect of Steam Reactivation. Figure 3 shows the decay curve of the HL

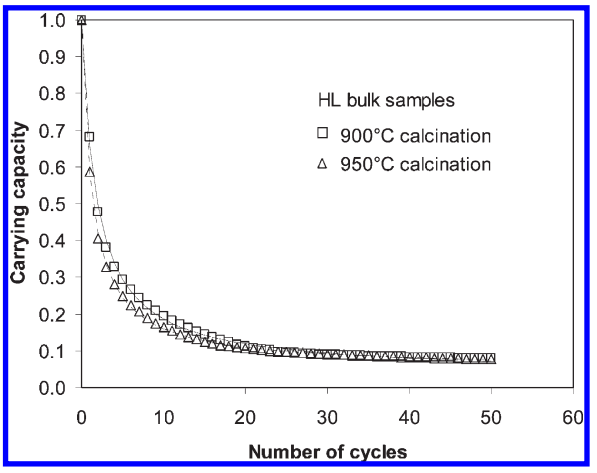

Figure 4. Effect of the calcination temperature on CO_2 carrying capacity for HL limestone (bulk sample). Calcination time, 5 min; carbonation temperature, 650 °C, for 5 min; p_{CO_2}, 0.015 MPa. The lines represent the data fitted with eq 2. From top to bottom: $k = 0.58$ and $X_\infty = 0.039$ (900 °C) and $k = 0.83$ and $X_\infty = 0.053$ (950 °C).

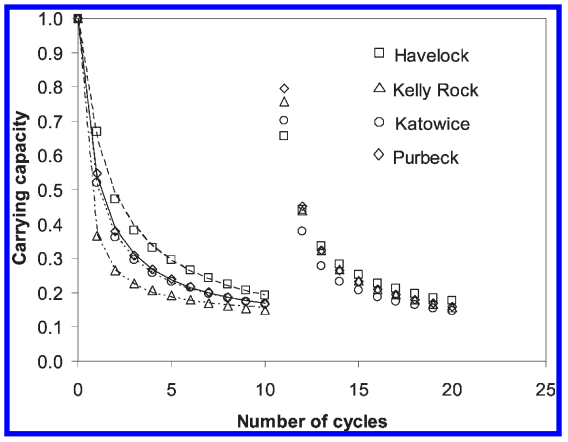

Figure 5. Effect of steam reactivation on four limestones (bulk samples). Calcination temperature, 900 °C, for 5 min; carbonation temperature, 650 °C, for 5 min; p_{CO_2}, 0.015 MPa; steam temperature, 130 °C (p_{CO_2}, 0.1 MPa), for 5 min. The lines represent the data fitted with eq 2. From top to bottom: $k = 0.63$ and $X_\infty = 0.057$ (HL), $k = 1.11$ and $X_\infty = 0.086$ (PB), $k = 1.28$ and $X_\infty = 0.097$ (KW), and $k = 2.90$ and $X_\infty = 0.122$ (KR).

sample and the effect of steam reactivation on CO_2 carrying capacity. The carrying capacity of a bulk sample degrades with the number of carbonation and calcination cycles, in agreement with literature results.[3,4,9−12,14−17] The carrying capacity reduced quickly in the first 10 cycles; however, the rate of decrease slowed after 10 cycles. The remaining carrying capacity after 30 cycles was about 10%. The steam reactivation after 10 cycles led to a significant increase (∼45%) in carrying capacity (from 20 to ∼65% for the bulk sample). Two single particle results (as shown in Figure 3) showed increases of 25 and 55% in carrying capacity (to ∼50 and 80%) after steam reactivation. A second steam reactivation was conducted on one of the single particles after 14 cycles (4 cycles after the first reactivation). The carrying capacity increased from 35 to 75% in the second reactivation, slightly less than after the first reactivation (from ∼25 to 80%). However, in all cases, the carrying capacity reduced quickly again after the reactivation.

A higher calcination temperature of 950 °C was tested on a bulk sample of HL limestone. In comparison to the calcination

Table 2. Comparison of Parameters before and after Steam Reactivation

	before reactivation			after reactivation		
limestone	X^a	d	ε	X^a	d	ε
HL	0.192	0.933[b]	0.815[b]	0.656	1.053[b]	1.164[b]
KR	0.148			0.757		
KW	0.166			0.701		
PB	0.166			0.795		

[a] Bulk samples. [b] Particle HL2, normalized results.

Table 3. Coefficients Used in the Grasa and Particle Shrinkage Equations

	Grasa equation (eq 2)		particle shrinkage equation (eq 3)	
limestone	k	X_∞	k_s	d_∞
HL	0.63	0.057	29	0.930
KR	2.90	0.122	110	0.987
KW	1.28	0.097	42	0.928
PB	1.11	0.086	88	0.988

at 900 °C, the higher calcination temperature resulted in about 10% lower reactivity (see Figure 4) in the first 5 cycles, which was possibly caused by enhanced sintering. The difference gradually diminished in the following cycles and vanished after about 20 cycles. Grasa and Abanades[14] observed that the decay in reactivity was drastically enhanced over 950−1000 °C. However, calcination temperatures over 950 °C were not employed in this work because of limitations of the apparatus, and all subsequent calcination tests were run at 900 °C.

Figure 5 shows the decay curves for bulk samples of four different limestones, illustrating that steam reactivation improves the CO_2 carrying capacity for each. Similar to the HL limestone, the carrying capacity of all limestones reduced quickly in the first 10 cycles, to about 20%, with a further gradual reduction to ∼6−12% after 50 cycles predicted by the Grasa equation (eq 2). Steam reactivation again resulted in a remarkable increase in the carrying capacity, from ∼20 to 65−80%. The carrying capacity changes for the four limestones before and after steam treatment are summarized in Table 2. It should also be noted that the carrying capacity again reduced quickly in the cycles after the steam reactivation, as shown in Figure 5. The coefficients used in the Grasa equation are shown in Table 3, which fit the experimental data very well.

The degree of hydration in steam reactivation or the hydration rate was studied by calcining the hydrated samples in the TGA in an inert environment while measuring the weight change. It was defined as the moles of CaO converted to $Ca(OH)_2$ divided by the moles of total available CaO. The hydration extent was between 90 and 95% in 1−10 min of steam reactivation at 130 °C (Figure 6). It was quite constant whether the steam reactivation was conducted after 10 or 20 cycles. Increasing the steam temperature to 160 °C or varying the reactivation time between 1 and 10 min had a marginal influence on the hydration extent. Previously, to restore the carbonation and/or sulfation potential of the sorbent, Fennell et al.[22] reactivated spent sorbents by exposing them to humid air overnight. They have demonstrated that overnight hydration and subsequent recalcination partially restored the volume inside the pores and increased the surface area substantially. Steam reactivation of spent sorbent from multiple CO_2 capture cycles was also investigated by Manovic et al.[18−21] A pressurized reactor was used in their

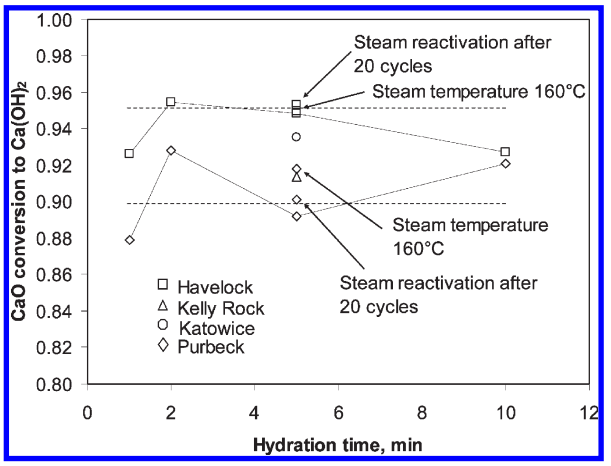

Figure 6. Hydration degree of the sorbent (bulk samples). Steam reactivation after 10 cycles. Steam temperature, 130 °C (p_{H_2O}, 0.1 MPa).

work. The sorbent was reactivated in high-pressure steam and/or for a longer period of hydration (15−60 min). However, because the hydration rate was studied for the first time after repeated cycles, the current work shows that steam reactivation is a rapid process and almost quantitative hydration (>90%) can be achieved in about 2 min with atmospheric pressure steam, even for cycled sorbents. This is an important finding, in that it shows that kinetic limitations for the use of hydration within a CaLC are much less than might have been inferred from previous work that used much longer hydration times. This obviously means that the treatment vessel can be smaller. However, it is important to note that even light sulfation might seriously impede the ability of the steam to rapidly rehydrate the particles, as well as the presence of impurities, such as ash, in a realistic setting.

Particle Size Change and Its Corresponding Influence on Porosity. *Particle Shrinkage*. Panels a and b of Figure 7 show the normalized particle linear length (diameter of the major axis) change during carbonation and calcination cycles for HL and KW limestones, respectively. These two limestones behaved similarly in terms of size change. The particle diameters reduced by ~7% after 4 cycles and showed little change in further cycles. It must be pointed out that the results for different particles for these two limestones are quite consistent and that panels a and b of Figure 7 are based on repeated tests on different particles. As also shown in panels a and b of Figure 7, the results of normalized length and normalized equivalent diameters were in good agreement. Therefore, only the results of normalized equivalent diameter are presented in panels c and d of Figure 7 for KR and PB particles, respectively.

KR and PB limestones showed much less shrinkage during carbonation and calcination cycles. For the KR limestone, the particle kept its original size or even swelled slightly after the first calcination. The particle size shrank less than 2% in diameter after 10 cycles. For the PB limestone, irregular results in particle size change were found. As shown in Figure 7d, particle PB1 had more size shrinkage (~2%) than particles PB2 and PB3, which showed only about 0.5% decrease in diameter after 50 cycles. The maximum shrinkage observed for the PB limestone was about 5% on particle PB4.

As a crosscheck for the consistency of the particle size change, KW and KR samples were rescreened to 0.71−0.8 mm, which is closer to the size range of the other two limestones. Additional tests were conducted on particles of this size range. As shown in panels b and c of Figure 7, the

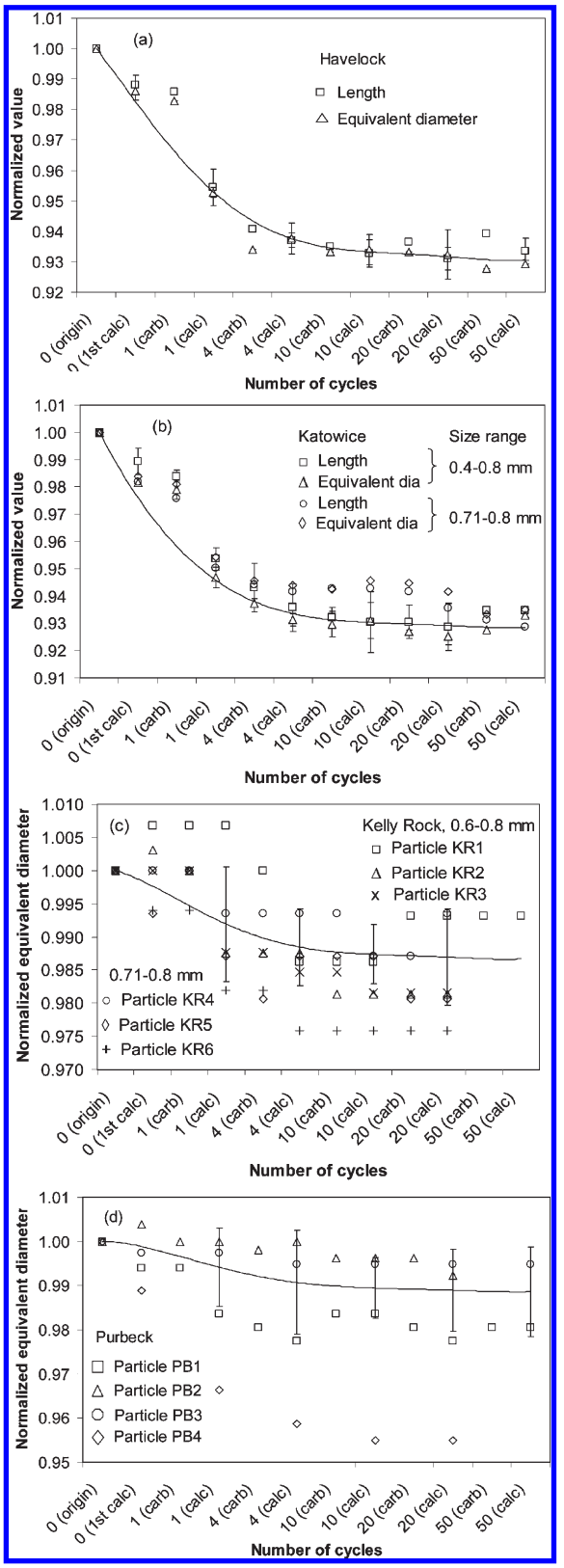

Figure 7. Particle size changes versus carbonation/calcination cycles: (a) HL, (b) KW, (c) KR, and (d) PB. Calcination temperature, 900 °C, for 5 min; carbonation temperature, 650 °C, for 5 min; p_{CO_2}, 0.015 MPa. The lines represent the normalized equivalent diameter data fitted with eq 3. From a to d: $k_s = 29$ and $d_\infty = 0.930$ (HL), $k_s = 42$ and $d_\infty = 0.928$ (KW), $k_s = 110$ and $d_\infty = 0.987$ (KR), and $k_s = 88$ and $d_\infty = 0.988$ (PB, average of particles PB1, PB2, and PB3).

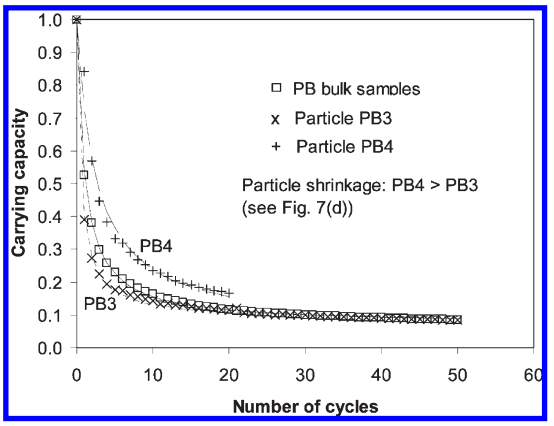

Figure 8. CO_2 carrying capacity versus the number of cycles (PB limestone). Calcination temperature, 900 °C, for 5 min; carbonation temperature, 650 °C, for 5 min; p_{CO_2}, 0.015 MPa. The lines represent the data fitted with eq 2. From top to bottom: $k = 0.42$ and $X_\infty = 0.050$ (PB4), $k = 1.06$ and $X_\infty = 0.070$ (bulk), and $k = 1.99$ and $X_\infty = 0.084$ (PB3).

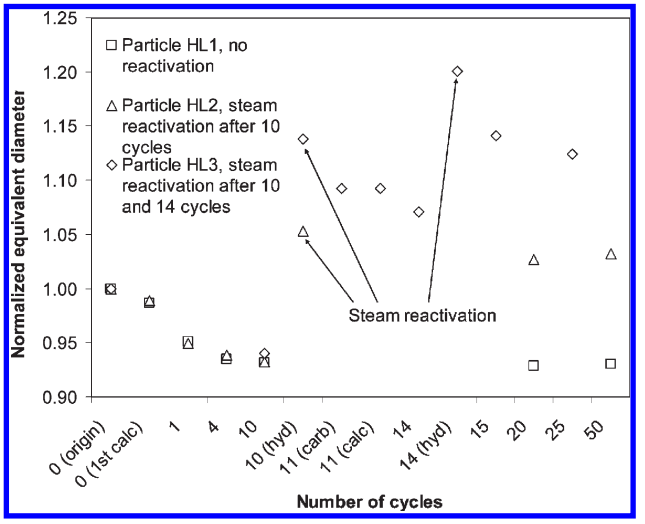

Figure 9. Particle size changes during carbonation/calcination cycles and steam reactivation (HL particles). Calcination temperature, 900 °C, for 5 min; carbonation temperature, 650 °C, for 5 min; p_{CO_2}, 0.015 MPa; steam temperature, 130 °C (p_{H_2O}, 0.1 MPa), for 5 min.

results for rescreened particles were consistent with those of the original size range.

The irregularity in particle size change, especially for the PB limestones, probably arose from the chemical composition of the original particles. As seen in Table 1, KR and PB had much higher SiO_2 content than HL and KW limestones (3−4 versus ~1%); further investigation showed that, for the PB limestone, the SiO_2 existed in the particle both as crystallites and in the form of flint (~200 μm). The flint appears to act as a "scaffold" to support the particle and prevent shrinkage during cycling. Of course, not every particle contained a flint, leading to the variability in the results for the PB limestone. It is also noted that the content of K_2O in KR and PB is higher than for the other samples and may have some effects on the sintering, although this is difficult to quantify precisely in a variable natural material, such as limestone, particularly with such small sample sizes.

It appears that the particle diameter reaches an asymptote after about 10 cycles, which is analogous to the decay in the

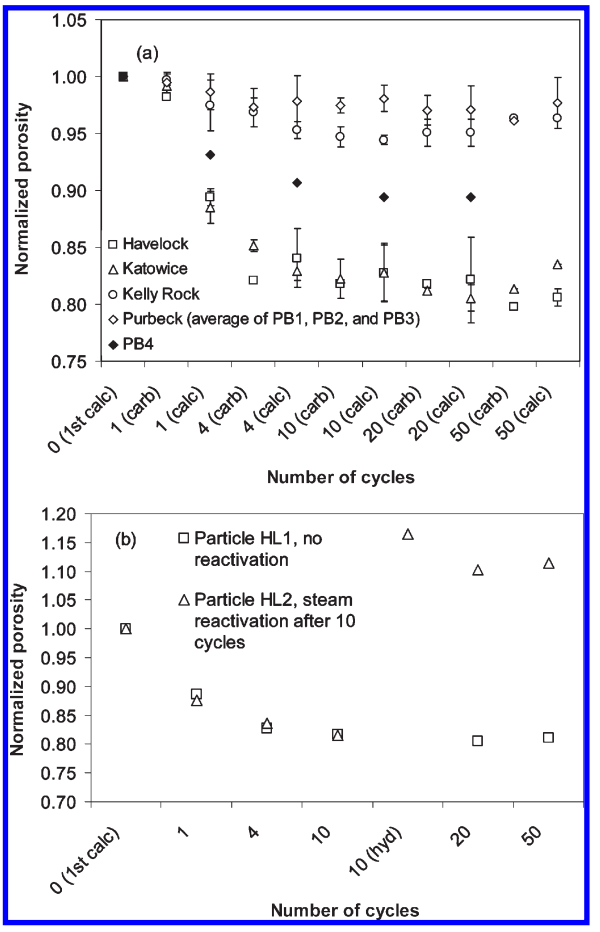

Figure 10. Particle porosity changes versus carbonation/calcination cycles: (a) four limestone particles and (b) HL (with steam reactivation). Calcination temperature, 900 °C, for 5 min; carbonation temperature, 650 °C, for 5 min; p_{CO_2}, 0.015 MPa; steam temperature, 130 °C (p_{H_2O}, 0.1 MPa), for 5 min. The porosity is calculated by eqs 4 and 5 with the equivalent diameter of the particle (shown in Figure 7).

carrying capacity of the limestone, expressed in eq 2. An empirical equation to describe the particle shrinkage may be proposed

$$d_N = \frac{1}{\frac{1}{1-d_\infty} + k_s N} + d_\infty \quad (3)$$

where d_∞ is the final particle size and k_s can be considered as a decay constant for the particle size. A greater value for k_s represents a smaller tendency for shrinkage. In Figure 7, the experimental data of particle diameters are fitted with eq 3, and the coefficients used in eq 3 are listed in Table 3.

When the reactivity decay (Figure 5) is compared to the particle size shrinkage (Figure 7) for the four limestones, it is interesting to note that the rate of decrease of the carrying capacity should be ranked as roughly HL < PB ≈ KW < KR, while the rank of size shrinkage can be roughly expressed as HL ≈ KW > PB ≈ KR. It is also interesting to note that, as well as the irregular results of the particle size change, the PB particles showed different performance in terms of CO_2 carrying capacity. As shown in Figure 8, PB4, which had a maximum size shrinkage among PB particles, had a better carrying capacity than particle PB3 (almost no shrinkage) and the average results represented by the bulk samples. This is probably because of the presence of one or

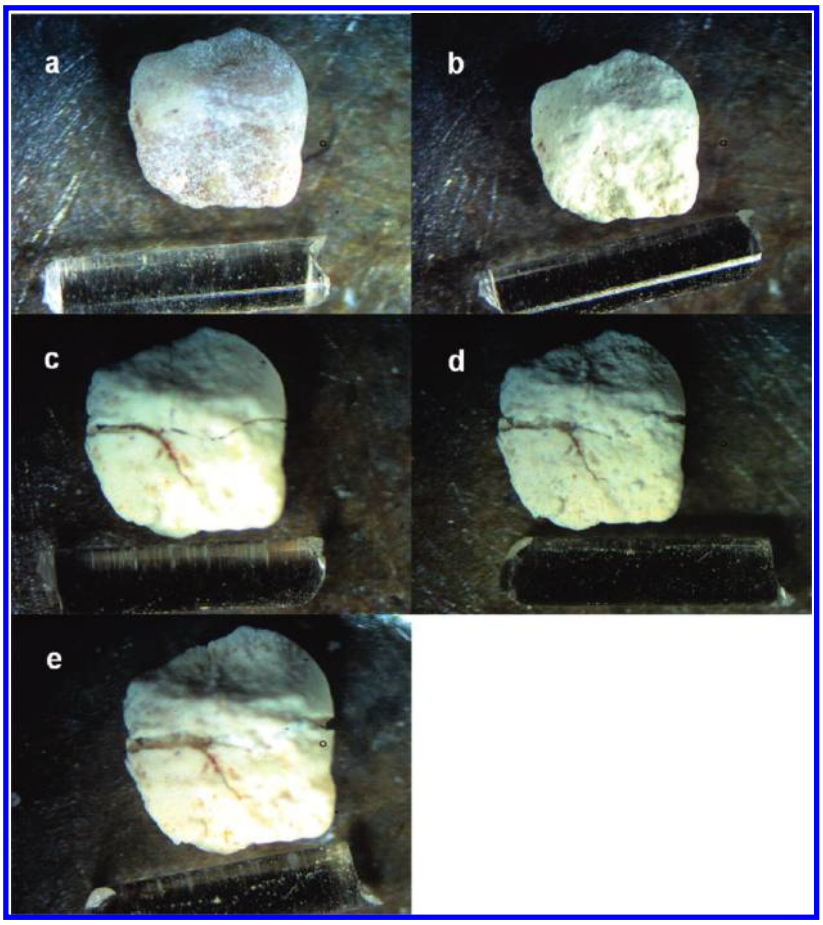

Figure 11. Optical microscope images of particles (magnification of 40×) at different calcination/carbonation cycles and steam reactivation: (a) original limestone particle, (b) 10 cycles, (c) steam reactivation after 10 cycles, (d) 4 more cycles after reactivation, and (e) second steam reactivation after 14 cycles. HL limestone particle; calcination temperature, 900 °C, for 5 min; carbonation temperature, 650 °C, for 5 min; p_{CO_2}, 0.015 MPa; steam temperature, 130 °C (p_{H_2O}, 0.1 MPa), for 5 min. The diameter of the quartz piece is 0.48 mm.

more inert flints present in particle PB3. Manovic et al.[23] have found in a recent study that, in multi-cycled sorbent particles, areas with greater SiO_2 content correlated with a smoother appearance in the SEM images. This suggested that SiO_2 is an unfavorable impurity affecting the surface area of the particle (i.e., enhancing sintering) and CO_2 carrying capacity; however, the exact form in which the SiO_2 is present (as either distinct flint particles or spread more continuously through the matrix of CaO) is probably important in determining how it affects the reactivity of a limestone.

Figure 9 shows the effect of steam reactivation on the particle size change for HL limestone particles. The particle size swelled ~12−22% in normalized equivalent diameter after reactivation and hardly changed during further cycles. Particle HL3 showed a little more swelling after a second reactivation, although little shrinkage of the particle was seen during further cycles.

The observed particle size reduction during the course of repeated carbonation and calcination cycles is important for modeling studies on particle behavior, particularly attrition.[24−26] For example, Saastamoinen et al.[26] studied the fragmentation and attrition of limestone particles in a fluidized bed. To simulate the evolution of particle size distribution as a result of thermal shock and during calcination, a population balance model was described in their work. However, the effect of calcination on particle size (particle shrinkage during calcination) was not taken into account in the particle size distribution equation. Figure 7 shows that the diameter of a particle changes by around 1−2% during first calcination for HL and KW limestones, although by much less for PB and KR limestone; this is probably not highly significant for systems involving only calcination. However, for similar studies involving repeated cycles (where we have shown here that there are substantial changes in particle size, independent of attrition effects), it is critical that changes in the particle diameter because of densification are correctly taken into account. The finding of this work indicates that any mathematical model proposed to simulate the transformation of limestone particles during realistic CaLCs, such as those in a fluidized bed reactor, will need to incorporate the contribution of particle size shrinkage upon repeated cycling, in addition to attrition. The extent to which particles shrink during repeated cycling also significantly

(24) Scala, F.; Salatino, P.; Boerefijn, R.; Ghadiri, M. Attrition of sorbents during fluidized bed calcination and sulphation. *Powder Technol.* **2000**, *107* (1−2), 153–167.
(25) Scala, F.; Salatino, P. Dolomite attrition during fluidized-bed calcination and sulfation. *Combust. Sci. Technol.* **2003**, *175* (12), 2201–2216.
(26) Saastamoinen, J.; Pikkarainen, T.; Tourunen, A.; Räsänen, M.; Jäntti, T. Model of fragmentation of limestone particles during thermal shock and calcination in fluidised beds. *Powder Technol.* **2008**, *187*, 244–251.

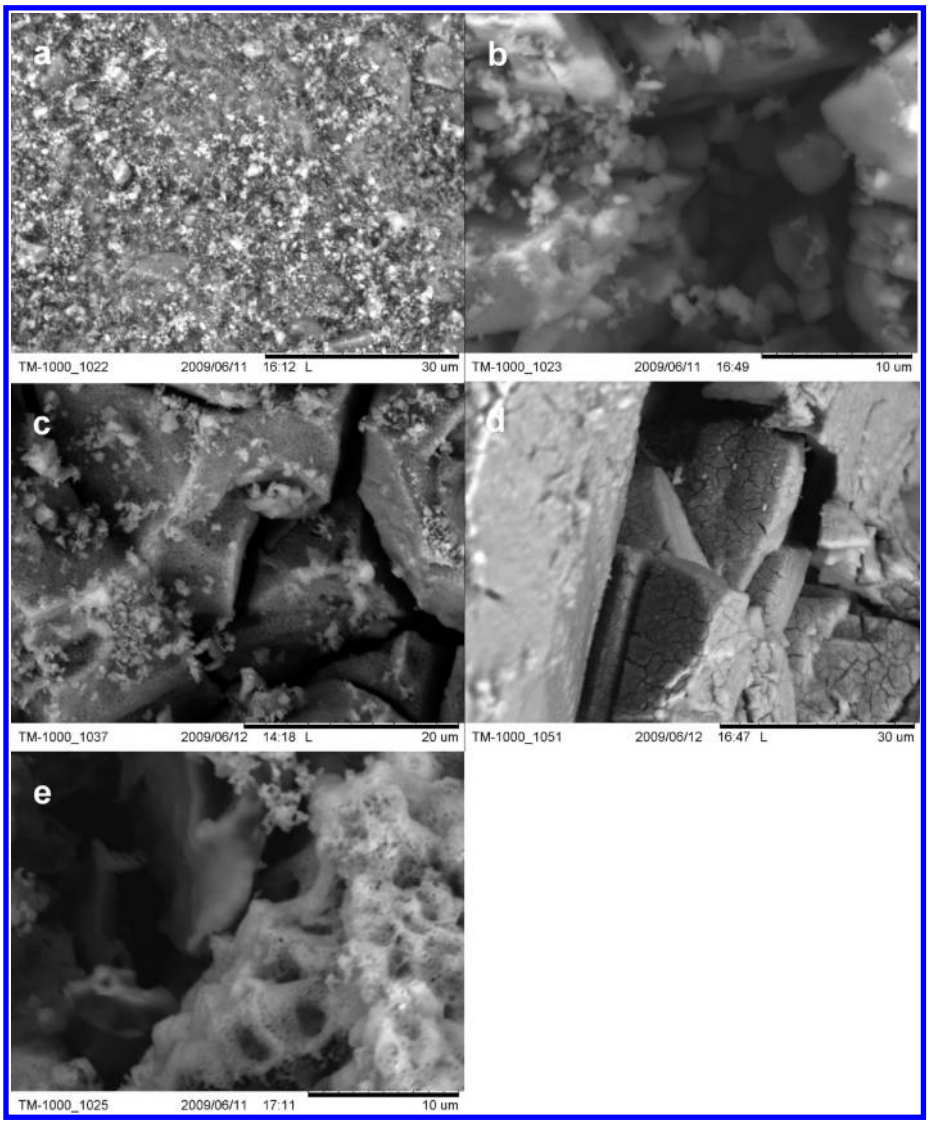

Figure 12. SEM photomicrographs of particles at different calcination/carbonation cycles and steam reactivation: (a) original limestone particle, $CaCO_3$; (b) first calcination, CaO; (c) 10 cycles, CaO; (d) steam reactivation after 10 cycles, $Ca(OH)_2$; and (e) 10 more cycles after reactivation, CaO. HL limestone particle; calcination temperature, 900 °C, for 5 min; carbonation temperature, 650 °C, for 5 min; p_{CO_2}, 0.015 MPa; steam temperature, 130 °C (p_{H_2O}, 0.1 MPa), for 5 min.

affects the propensity of particles to break apart during or after the use of hydration to reactivate them.[27]

Calculation of Porosity. The porosity of the particle after the first calcination can be calculated by assuming that the number of moles of $CaCO_3$ and CaO, before and after calcination, is equal. For a spherical particle, eq 4 can be derived

$$\frac{4}{3}\frac{\pi {r_0}^3 \rho_{CaCO_3}(1-\varepsilon_0)}{M_{CaCO_3}} = \frac{4}{3}\frac{\pi {r_c}^3 \rho_{CaO}(1-\varepsilon_c)}{M_{CaO}} \quad (4)$$

where ρ and M are density and molar weight, respectively, r_0 is the initial particle radius, ε_0 is the porosity of the limestone particle, r_c is the radius after first calcination, and ε_c is the porosity of the fresh calcined particle.

The natural porosity of limestone is normally quite low. In this work, the original limestone particle is assumed here to be non-porous (i.e., $\varepsilon_0 = 0$). Following the first calcination, eq 5 can be derived from molar conservation of CaO between the carbonation/calcination cycles[28]

$$\varepsilon_t = 1 - \left[\frac{r_c}{r_t}\right]^3 (1-\varepsilon_c) \quad (5)$$

where r_t is the radius of the particle at time t and ε_t is the porosity of the particle at time t.

Equation 5 indicates that the porosity, ε_t, is a function of the cube of the particle diameter and that the small changes in particle size observed in this work lead to substantial changes in their porosity. Such findings are important for calculations of, e.g., the effectiveness factors of particles. They are also important when modeling the growth of carbonate in such particles.

With the particle size measured in this study, the porosity of the particle, ε_c and ε_t, can be calculated with eqs 4 and 5, respectively. The average porosities of fresh calcined limestone,

(27) Blamey, J.; Paterson, N. P.; Dugwell, D. R.; Stevenson, P.; Fennell, P. S. *The reactivation of CaO based sorbent for CO_2 capture from combustion and gasification plants*. Proceedings of the Combustion institute (34th Symposium), manuscript submitted.

(28) Warren, T.; Mumby, W. Final year report investigating the change in macro particle size during CaO looping for the purposes of CO_2 capture. Imperial College London, London, U.K., 2008.

ε_c, for the four samples investigated were calculated: HL, 0.507 ± 0.004; KR, 0.531 ± 0.005; KW, 0.500 ± 0.0004; and PB, 0.521 ± 0.0090. Because the porosity of a freshly calcined particle, ε_c, is different from particle to particle, the normalized results are given in Figure 10 for the purposes of comparison. Figure 10a shows that both HL and KW particles had a significant decrease, 15−20%, in porosity in the first 4 cycles. There was a smaller decrease in porosity (< 5%) for KR and PB limestones. The porosity of different PB particles showed inconsistent results, as would be expected from the size change results. The porosity of particle PB4 reduced about 10% after 10 cycles, which is the greatest among the PB particles tested. In Figure 10b, the porosity of a HL particle increased markedly after steam reactivation. This is because the particle swelled and cracks formed after hydration. The diameter and porosity (normalized values) changes for HL samples before and after steam reactivation are shown in Table 2.

Optical Microscope and SEM Photomicrographs. Figure 11 shows photomicrographs during cycles of calcination and carbonation and after steam reactivation. It is clearly visible that the particle shrinks after 10 cycles (Figure 11b) when compared to the original size (Figure 11a). After steam hydration (Figure 11c), cracks can be seen on the surface of the particle. During the following cycles, the particle shrinks again as the cracks become wider (Figure 11d) but the particle size does not recover to the previous size before reactivation. The second reactivation causes the cracks to grow even larger (Figure 11e), and the size of the particle swells again.

Figure 12 shows SEM photomicrographs during the carbonation/calcination cycles and after steam reactivation. The limestone particle calcines from a relatively non-porous material ($CaCO_3$; Figure 12a) to an extremely porous solid (CaO; Figure 12b), with a pore size of 2−3 μm. After 10 carbonation/calcination cycles, the grain size becomes larger (~10 μm) with some cracks on the surface (CaO; Figure 12c) but the interior of the cracks looks smoother. After steam reactivation, crystals of $Ca(OH)_2$ can be seen in Figure 12d. Figure 12e shows a smoother interior again (CaO) after 10 more cycles.

Conclusions

Carbonation and calcination cycles were carried out on four limestones in a TGA apparatus, and the spent sorbents were reactivated with steam in a steam hydrator at atmospheric pressure. The CO_2 carrying capacity of a limestone particle decays very quickly in the first 10 cycles. The remaining carrying capacity reduces to 6−12% after 50 cycles for the four limestones studied in this work. The diameters of limestone particles shrink by ~7% after about 4 cycles for HL and KW samples, equivalent to a ~20% reduction in the porosity. KR and PB particles show much lower tendency for shrinkage (~2%), and PB particles have quite irregular results, ranging from very little size change to a maximum of 5% found for one particular particle. Steam reactivation after 10 cycles results in an immediate increase (by 45−60% points) in carrying capacity and an almost quantitative formation of $Ca(OH)_2$ within 5 min, indicating that hydration is a relatively fast process. The particle size and the corresponding porosity can be increased after reactivation because of the formation of cracks. The finding of particle size reduction during repeated cycles is important for attrition studies of the CaLC and for the development of detailed models of carbonation.

Acknowledgment. The authors are grateful for the financial support from King Abdullah University of Science and Technology (KAUST), in conjunction with the Department of Chemical Engineering at Imperial College London, and from Canmet-ENERGY, Natural Resources Canada.

Nomenclature

d_N = particle size after the Nth cycle (m)
d_∞ = final particle size (m)
k = deactivation constant
k_s = decay constant for the particle size
M = molar weight (kg/mol)
N = cycle number
r_0 = initial particle radius (m)
r_c = radius after first calcination (m)
r_t = radius of the particle at time t (m)
t = time (s)
X_N = carrying capacity after the Nth cycle
X_∞ = residual carrying capacity

Greek Symbols

ε_0 = initial porosity of the limestone particle
ε_c = porosity of the fresh calcined particle
ε_t = porosity of the particle at time t
ρ = density (kg/m^3)